Click Here for Full Article

Effect of 1998 El Niño on the distribution of phytoplankton in the South China Sea

Hui Zhao[1] and Dan Ling Tang[1]

[1] The present study analyzed interannual variation of phytoplankton/Chlorophyll-a (Chl-a) distribution in the South China Sea (SCS) for the period from 1997 to 2005 using SeaWiFS-derived Chl-a data and other oceanographic data. The results show high spatial variation of Chl-a concentrations in the SCS and revealed an anomalous event in 1998. High Chl-a concentrations in the southwestern SCS in the summer season (June to August) may be related with strong Ekman Pumping and strong wind stress, whereas a jet-shape high Chl-a region offshore in western SCS was associated with coastal upwelling driven by offshore Ekman transport and Vietnamese offshore current. Chl-a concentrations in 1998 summer in the SCS were the lowest among the 7 years and were particularly low in the western SCS. At the same season, the jet-shape Chl-a region offshore of southeast Vietnam almost disappeared, and southwesterly monsoon winds and offshore current were relatively weaker in 1998. This anomalous event of low phytoplankton biomass in the SCS coincided with an El Niño year in 1998.

1. Introduction

[2] The biological processes in the ocean are largely controlled by the phytoplankton biomass because phytoplankton forms the basis of food chain and affects sea surface CO_2 through photosynthesis. Taking the advantage of remote sensing technology, the present study investigated the interannual variation of phytoplankton distribution in the South China Sea (SCS), aiming to better understand marine ecosystems related with oceanic environments, particularly with El Niño effects, in this region.

[3] The SCS, located in the western Pacific Ocean (Figure 1), is one of the largest marginal seas in the world. It covers 3.5 million km^2 from the equator to 23°N and from 99°E to 121°E with an average depth of 2000 m. The East Asian monsoon plays an important role in hydrological features and upper layer circulations of SCS [*Wyrtki*, 1961; *Lau et al.*, 1998]. In summer (June-August), when southwesterly monsoon winds prevail [*Yang and Liu*, 1998; *Liu and Xie*, 1999], the orientation of the coastline provides favorable conditions for wind-induced upwelling roughly along the west coastline and offshore currents in the SCS [*Shaw and Chao*, 1994; *Chu et al.*, 1998; *Xie et al.*, 2003]. Those oceanographic conditions exert important impacts on the dynamics of marine ecosystems for the northwestern SCS and even the entire SCS [*Tang et al.*, 2004a, 2004b].

[4] Previous studies on phytoplankton dynamics have been conducted for different regions of the SCS [*Hung and Tsai*, 1984; *Agawin et al.*, 2003]. *Lee Chen et al.* [2004] investigated influence of nitrogen on phytoplankton growth in spring in the SCS with in situ data. *Tang et al.* [1998, 1999, 2003, 2004a, 2004b] reported winter phytoplankton blooms in Luzon Strait and the Gulf of Tonkin related with winter upwelling, offshore increase of phytoplankton biomass in the southeast Vietnamese coastal water related with summer southwest monsoon wind, and harmful algal bloom in northern SCS. *Liu et al.* [2002] studied Chl-a distribution and primary production in SCS using monsoon-forced numerical model. They found an evident vertical distribution in Chl-a and primary production, which is a strong seasonal feature in the summer in the SCS in three upwelling regions including the offshore the east coast of Vietnam. *Lin et al.* [2003] speculated that typhoon events would triggered marine phytoplankton blooms, whereas *Vo and Hodgson* [1996] and *Vo* [1998] described Vietnam's nearshore reefs and the diversity of corals, investigating the relation between the distribution of coral reefs and species in Vietnam and biological and environmental conditions. In addition, previous studies [*Tang et al.*, 2003, 2004b; *Zhao et al.*, 2005b] indicate that SeaWiFS derived Chl-a values match survey measurements in most area of the SCS, and SeaWiFS Chl-a values are higher than the survey measurements near the Mekong River Estuary and Hainan Island. Despite these studies, however, little has been known about the effects of El-Nino on the distribution of Chl-a concentrations in the SCS.

[5] In the present study, we investigated spatial-temporal variations of Chl-a concentrations during the summer season for the entire SCS using a suite of satellite products, i.e.,

---

[1]Remote Sensing of Marine Ecology and Environment Group (RSMEE), Laboratory for Tropical Marine Environmental Dynamics, South China Sea Institute of Oceanology, and Graduate School of Chinese Academy of Sciences, Chinese Academy of Sciences, Guangzhou, China.
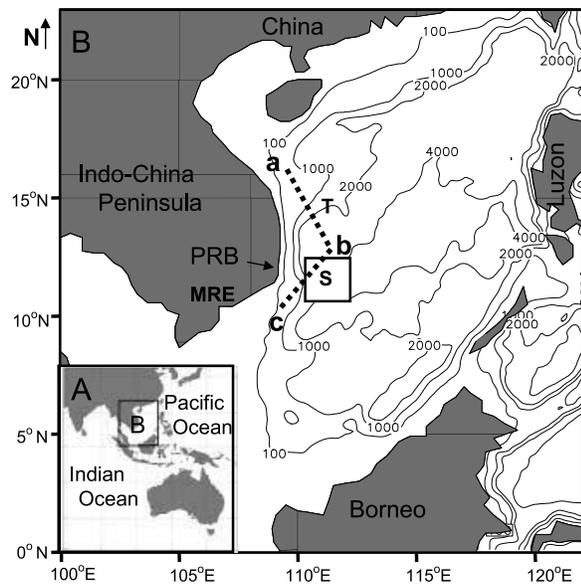
Figure 1. (a) Location of study area the South China Sea (SCS). (b) Bathymetric and geographic map of the SCS. Box S: a sampling region of SeaWiFS Chl-a; Transect T (a-b-c): sampling transect crossing upwelling areas. PRB, Phan Ri Bay; MRE, Mekong River Estuary.

Chl-*a* concentrations, Sea Surface Temperature (SST), sea surface winds, Ekman Pumping velocity besides historical in situ investigations. We subsequently discussed reasonable environmental mechanisms underlying the observed variations in Chl-*a*. Our study mainly focused on the western SCS where there are complex hydrographic conditions and ecosystems as mentioned above. We have found interesting phenomena responsible for interannual variation in Chl-*a* distribution. These phenomena were especially marking for 1998 that is the most intense El Niño year with anomalous high SST, weak wind and weak wind-driven ocean circulations in the 20th century [*Xie et al.*, 2003]. This El Niño may have substantially influenced marine ecology in the SCS. Abnormal phytoplankton activities in 1998 were emphasized while presenting annual phytoplankton activities for the SCS.

2. Study Area, Data and Methods

2.1. Study Area and Data Sampling

[6] The SCS is a marginal sea of the west Pacific Ocean, located in the tropical east-Asia monsoon zone between the Equator and the Tropic of Cancer (Figure 1a). Our study area is mainly situated in the western SCS with wide continental shelf south and north of the SCS. There is relatively narrow continental shelf in the western region near Phan Ri Bay (Figure 1), where the depth reaches 500 m in 20 km from the coastline at its narrowest.

2.1.1. Satellite Images for the SCS for Four Periods

[7] In the following data processing, all kinds of data, including Chl-*a*, SST, sea surface wind stress (SSWS), and the Ekman pumping velocity (EPV) for the summer season (1 June – 31 August) were averaged from the monthly data. To reveal the special variation in 1998, all kinds of data were processed for 4 periods: (i) 1998–2004; (ii) 1999–2004; (iii) 1998; (iv) a period as long as data are available.

Because SeaWiFS was launched in September 1997, Chl-*a* data are only available for (i), (ii) and (iii) three periods.

2.1.2. Time Series Data for Upwelling Area

[8] Box S (Box S in Figure 1) is a small rectangular area (11–12.6°N and 110–112°E), in which an offshore jet current occurs generally in almost every summer [*Xie et al.*, 2003; *Tang et al.*, 2004a, 2004b]. To display annual recurrence of the high Chl-*a* in the western SCS, a time series data of monthly Chl-*a* were averaged spatially from Box S. We also quantitatively analyzed time series data of Chl-a, SST, SSWS and EPV for the summers (averaged for 1 June – 31 August) from 1998 to 2004.

2.1.3. Time Series Data Along the Vietnamese Coastline

[9] Transect T (a-b-c in Figure 1) (a: 16°N, 110°E; b: 12.5°N, 111.75°E; c: 10°N, 109.5°E) is designed for data sampling across the upwelling region along the Vietnamese coastline. One time series of monthly Chl-*a* data from June 1998 to July 2005 was processed along this latitudinal section T. At the same time, SSWS and SST data along T were processed into the Latitude-time image on the basis of monthly wind stress data from September 1997 to December 2003 and monthly SST data from September 1997 to December 2004.

2.2. SeaWiFS-Derived Chl-a Data

[10] Sea-viewing Wide Field-of-view Sensor (SeaWiFS) is on board the SeaStar spacecraft of NASA (National Aeronautics and Space Administration, United States). It has been in operation since August 1997. In the present study, the data acquired from SeaWiFS v.4 were used to derive the Chl-*a* concentrations. Level 3 Monthly Standard Mapped Image (SMI) data were interpolated to a regular grid of equidistant cylindrical projection of 2160×4320 pixels (about 9.2 km), from October 1997 to July 2005. The data were obtained from the Distributed Active Archive Center (DAAC) of Goddard Space Flight Center (GSFC), NASA (http://oceancolor.gsfc.nasa.gov/cgi/level3.pl).

2.3. Ocean Environmental Data

#### 2.3.1. Sea Surface Wind Stress (SSWS)

[11] The monthly wind stress data entitled Tropical Indian Winds were obtained from the Center for Ocean-atmospheric studies of Florida State University (http://www.coaps.fsu.edu). The data were pseudo-stressed based on surface marine observations (TD-1129) and the COADS CMR5 individual ship measurements made by NCDC (National Climatic Data Center), with 1° resolution of expressed in $m^2 \cdot s^{-2}$. We have obtained data for the period from January 1970 to December 2003.

2.3.2. Sea Surface Temperature (SST)

[12] SST data from Advanced Very-High Resolution Radiometer (AVHRR) Pathfinder Version 5 SST Project (spatial resolution 4 km/month-daytime), which is a new reanalysis of AVHRR data stream, were obtained from Physical Oceanography Distributed Active Archive Center (PO.DAAC), Jet Propulsion Laboratory (JPL), NASA (http://podaac.jpl.nasa.gov/sst). The monthly average products for 1985–2004 are used in present study.

2.3.3. Ekman Pumping Velocity

[13] The Ekman pumping velocity is an important index of vertical movements in oceans; it can help understand the
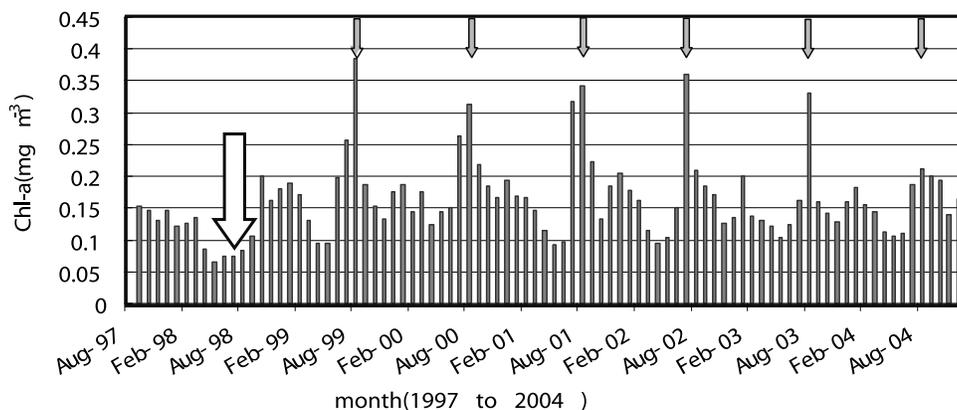
Figure 2. The time series of Chl-*a* concentrations averaged for Box S (S in Figure 1b). X-axis represents yearly dates (month). Grey arrows point to August from 1999 to 2004 with the maximum Chl-*a*. White arrow points to June to August for 1998.

distribution of Chl-*a* in the study area. The velocity can be calculated from the equation [*Stewart*, 2002]

$$W = -\text{Curl}(T \bullet \rho^{-1} \bullet f^{-1}), \qquad (1)$$

where W is the Ekman pumping velocity, T, ρ and f are respectively wind stress, sea water density and the Coriolis parameter. Given the wind stress data, we can easily obtain the Ekman pumping data from equation (1). In this study, Ekman pumping velocity data were processed into monthly data based on the longtime NCEP monthly wind data (1970–2003) through equation (1).

3. Results

3.1. Distribution of Phytoplankton

3.1.1. Monthly Variation of Chl-*a*

[14] The time series of Chl-*a* concentrations (Figure 2) averaged for Box S (S in Figure 1) represents the monthly variation of Chl-*a* during September 1997 to December 2004 and shows high concentrations (≥ 0.2–0.35 mg m^{-3}) in summer and low concentrations (≤ 0.1 mg m^{-3}) in spring. The maximum of monthly Chl-*a* concentrations

typically occurred in August/July every summer (black downward arrows in Figure 2), while the minimal Chl-*a* concentrations mainly occurred in April/May every spring. However, we noticed that the Chl-*a* concentrations were very low in the summer of 1998 (a white downward arrow in Figure 2). The Chl-*a* concentrations were only about 0.065 mg m^{-3} in July and August of 1998, much lower than the level of 0.25 mg m^{-3} for the same months of typical years.

3.1.2. Interannual Variation of Summer Chl-*a* in the SCS

[15] The comparison of Chl-*a* distributions in the summer season of three periods: 1998–2004 (Figure 3a), 1999–2004 (Figure 3b) and 1998 (Figure 3c) revealed obvious differences among those periods. Chl-*a* concentrations for the summer of 1998 (Figure 3c) were lower than the average for 1998–2004 (Figure 3a) and much lower than the average for 1999–2004 (Figure 3b). These differences were especially evident in the western SCS. In the following analysis, we therefore take 1999–2004 (Figure 3b) as general years and 1998 (Figure 3c) as a special year.

[16] Relatively high Chl-*a* concentrations (≥ 0.13 mg m^{-3}) were observed in open sea basin western SCS (white oval
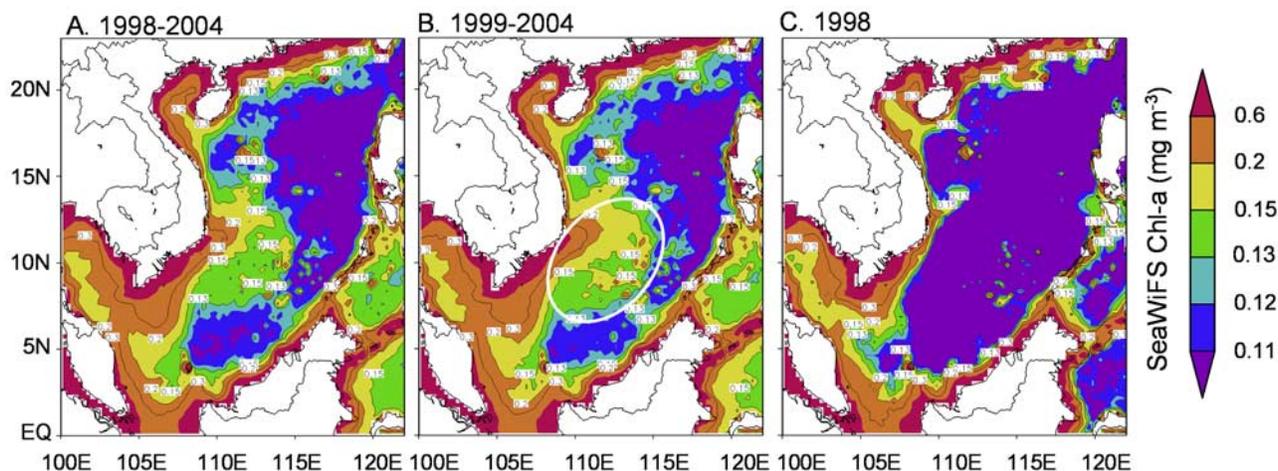
Figure 3. Summer (averaged for 1 June – 31 August) SeaWiFS-derived Chl-*a* images in the SCS.
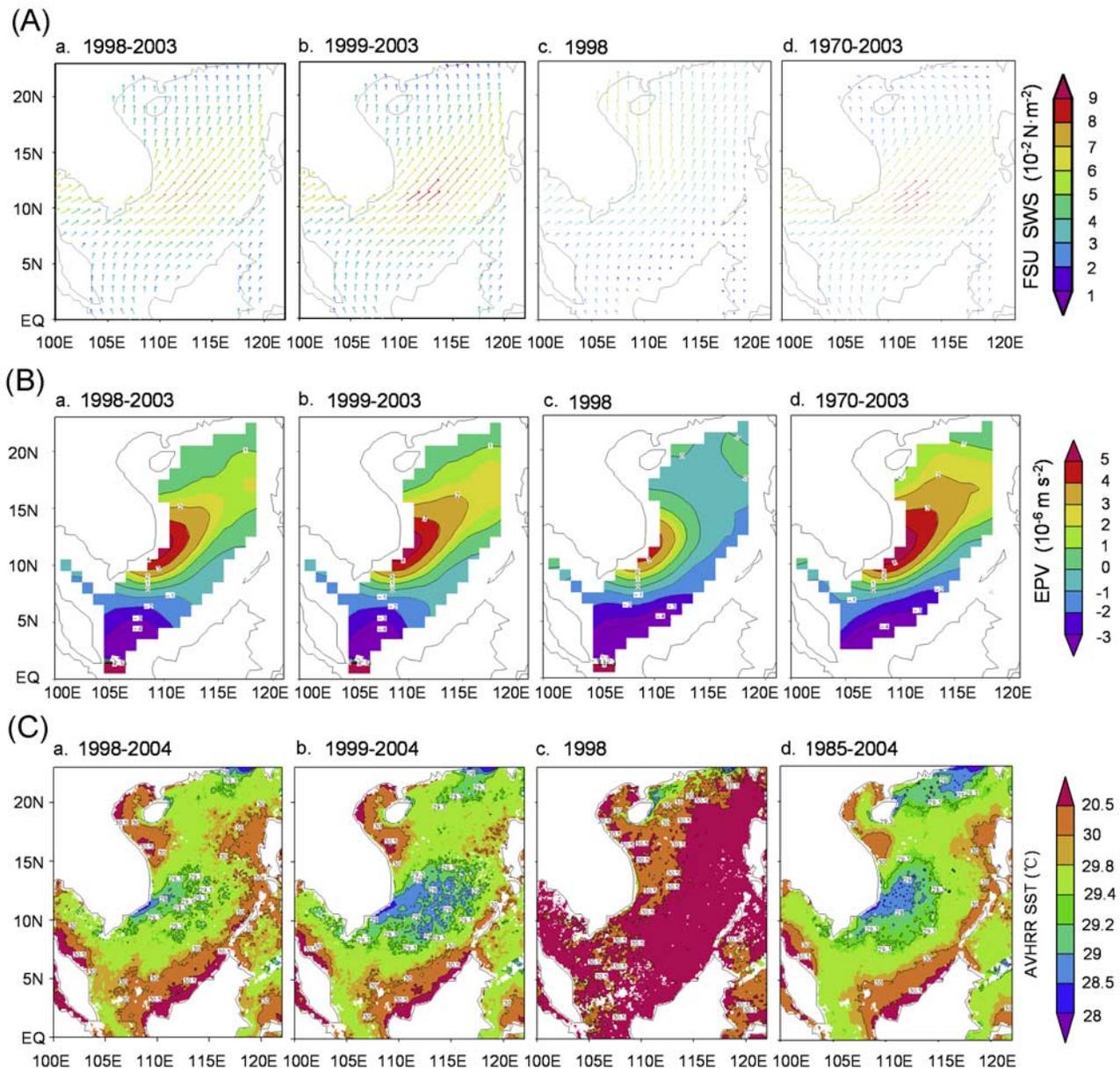
Figure 4. (a) Summer (averaged for 1 June – 31 August) FSU SSWS vectors and their magnitude (color shade in 10^{-2} N m^{-2}); (b) summer (averaged for 1 June – 31 August) Ekman Pumping velocity (upward positive in 10^{-6} m/s) in the SCS; (c) AVHRR summer (averaged for 1 June – 31 August) Sea Surface Temperature Images in the SCS (shaded in °C).

area in Figure 3b); however, low Chl-*a* concentrations presented (≤ 0.1 mg m^{-3}) in large regions, such as northeastern (excluding coastal waters) SCS and northwestern Philippine Islands. An extremely high band of Chl-*a* (≥ 0.2 mg m^{-3}) were observed parallel to the coastline within the range of 200 km from Mekong estuary to the Phan Ri Bay. A high Chl-*a* band extended offshore from near Phan Ri Bay up to 116°E, forming a "Chl-*a* jet."

[17] In the summer of 1998, Chl-*a* concentrations (Figure 3c) were lower, compared with the Chl-*a* level for general summers in most areas of SCS (≤ 0.1 mg m^{-3}) and were particularly low in the western SCS. The coastal band of high Chl-*a* concentrations was limited to a very narrow

and small range. In addition, the jet-shape offshore Chl-*a* region, which appeared in summer of general years, almost disappeared in 1998 summer.

3.2. Environmental Factors

3.2.1. Sea Surface Wind Stress (SSWS) and Ekman Pumping

[18] Spatial patterns of SSWS distribution were similar for 1998–2003 and 1999–2003 (Figure 4), while SSWS was weaker for 1998–2003 than for 1999–2003 (Figure 4) and SSWS speeds were even weaker for 1998 summer (Figure 4). The summer wind stress of climatology of SSWS averaged from 1970 to 2003 (Figure 4) reached maximum (~ 0.09 Nm^{-2}) around 11°N off Vietnam, that

almost doubles the stress averaged for the whole SCS. The axis of the wind stress (Figure 4) is roughly in the direction of northeastern Phan Ri Bay, dividing SCS into two parts.

[19] The Ekman pumping velocity displayed similar spatial pattern of weak/strong wind stress during the corresponding period: Ekman pumping appeared weaker in 1998–2003 than in 1999–2003 (Figure 4). In open sea basin southwest of the SCS, strong Ekman pumping induced by wind stress curls was represented (Figure 4) which induces seawater upwelling (called "Ekman upwelling" hereafter). However, during the summer of 1998 (Figure 4), the tendency of upwelling was very weak and associated to the anomalous weakening wind stress. On the other hand, the climatologies of SSWS and Ekman pumping velocity (Figure 4) showed also strong wind speed and strong Ekman upwelling west of the SCS (i.e., southeast of Vietnam) in the summer of usual years. On the northern areas of the axis of the wind stress, Ekman upwelling prevailed, compared with Ekman downwelling on the south of the axis (Figure 4).

3.2.2. Spatial Variation of SST

[20] The spatial distributions of summer SST (Figures 4) were also significantly different among 1998–2004, 1999–2004 and 1998. SST for 1998 summer was approximately 0.5–3°C, higher than other years (Figure 4). Summer SST (Figure 4) for 1999 to 2004 presented high temperature ($\geq$29.5°C) in most areas of the SCS and low temperature ($\leq$29.3°C) in the scope of ellipse (i.e., the location of the oval in Figure 3b) with a short radius of rough 500 km southeast of Vietnam in the western SCS. This pattern roughly matches the high positive Ekman pumping velocity (Figure 4) and the strong wind stress.

[21] An offshore jet-shape of lower SST ($\leq$29°C) in the northeast of Phan Ri Bay and a coastal band of lower SST in coastal regions in the southeast of Vietnam were observed in the summer of 1999–2003 and 1985–2004 (Figure 4). This jet-shape feature, however, almost disappeared in 1998 (Figure 4). In 1998, SST was consistently higher ($\geq$30°C) with the band of low SST along the southeast Vietnam being smaller and narrower compared with other years.

3.3. Variation of Chl-a and Environmental Conditions Along Section T

[22] Chl-*a* concentrations along transect T (Figure 1) displayed seasonal and annual cycle in the Vietnamese upwelling areas (Figure 5a), reaching a maximum in summer monsoon and a minimum in spring. High Chl-*a* concentrations ($\geq$0.12 mg m^{-3}) generally appeared between 10°N $\sim$ 14°N (i.e., summer upwelling area in the western SCS) in summer for almost every year, especially in 2000. However, in 1998 Chl-*a* concentrations were very low ($\leq$0.1 mg m^{-3}) during the entire year, especially in the summer.

[23] Seasonally reverse monsoon wind is clearly presented along transect T (Figure 5b): strong northeasterly wind prevailed in winter, strong southeasterly wind in summer, and weak wind in autumn and spring. However, in 1998, summer wind in the upwelling area (white rectangular area in Figure 5b) was the weakest among the 7 years (arrow 1 in Figure 5b).

[24] SST (Figure 5c) was low in winter and high in spring and summer in the SCS. During the summer, relatively low SST appeared in the high Chl-*a* area (10°N$\sim$14°N, i.e., white box in Figure 5b) compared to the ambient areas. Therein, the characteristic of low SST (Figure 5c) in 2000 was more distinct than in other years, no matter in winter or summer. In 1998, SST was the highest among the 7 years for the entire SCS; and the relatively low temperature region (between 10–14°N), which appears almost for every year, did not appear in 1998 summer.

3.4. Annual Variation of Chl-a, SST and Oceanography Data on Box S

[25] The time series (Figure 6) showed the relationship among Chl-*a* and other oceanographic factors sampled from Box S (11–12.6°N and 110–112°E, Figure 1). The Chl-*a* concentration is low in 1998 (0.0791 mg m^{-3}), while high SST (30.4574°C) and weak SSWS (0.05037 N m^{-2}) and EKP (0.2311 m/day) were observed in the same year.

4. Discussion

[26] In general, the availability of nutrients and light radiation are two key factors limiting the development and growth of phytoplankton. For our study area in the SCS, the sunlight illumination is not a limiting factor as this area locates in the tropics, but the accessibility of nutrients can be the determining factor [*An and Du*, 2000; *Tang et al.*, 2003, 2004a]. Therefore, complex hydrological conditions in the study area must have a considerable influence on the phytoplankton growth, by means of affecting the transportation and distribution of nutrient-rich water.

4.1. High Chl-a Concentrations in the Western SCS

[27] The sea surface Chl-*a* displayed a great spatial variation with high Chl-*a* concentrations in the southwestern SCS (8–14°N & 109–116°E). The depth of the region is over 1500 m and is about 40 km away from the coastline and over 300 km from Mekong estuary. The direct influence of freshwater runoff and coastal nutrients thus may be very minor. According to our results, the strong wind stress (Figure 4) alongshore can induce upwelling from beneath mixed layer to the surface in the coastal areas along the southeast of Vietnam. In this case, coastal upwelling may play an important role in providing nutrients for phytoplankton. Previous studies also revealed high Chl-*a* concentrations in summer [*Tang et al.*, 2004a, 2004b], where offshore high Chl-*a* was induced by the coastal upwelling and anticyclonic circulations [*Shaw and Chao*, 1994; *Xie et al.*, 2003; *Tang et al.*, 2004a].

[28] In the present study, we observed strong offshore Ekman Pumping (Figure 4) in the region of high Chl-*a* concentrations, where depth is over 500 m (Figure 3b). In this region, coastal upwelling, tidal mixing and river discharge may not be strong enough to provide rich nutrients into this euphotic zone. In this situation, Ekman upwelling brought up cold waters with rich nutrients (Figure 4) to provide offshore high Chl-*a* in the western SCS. The existence of SST low water mass in the western SCS also indicated strong Ekman upwelling (Figure 4). The summer anticyclonic circulation then may enhance the tendency of offshore high Chl-*a*.

[29] However, at the same time, the strong wind stress (Figure 4) makes also violent mechanical mixing for the
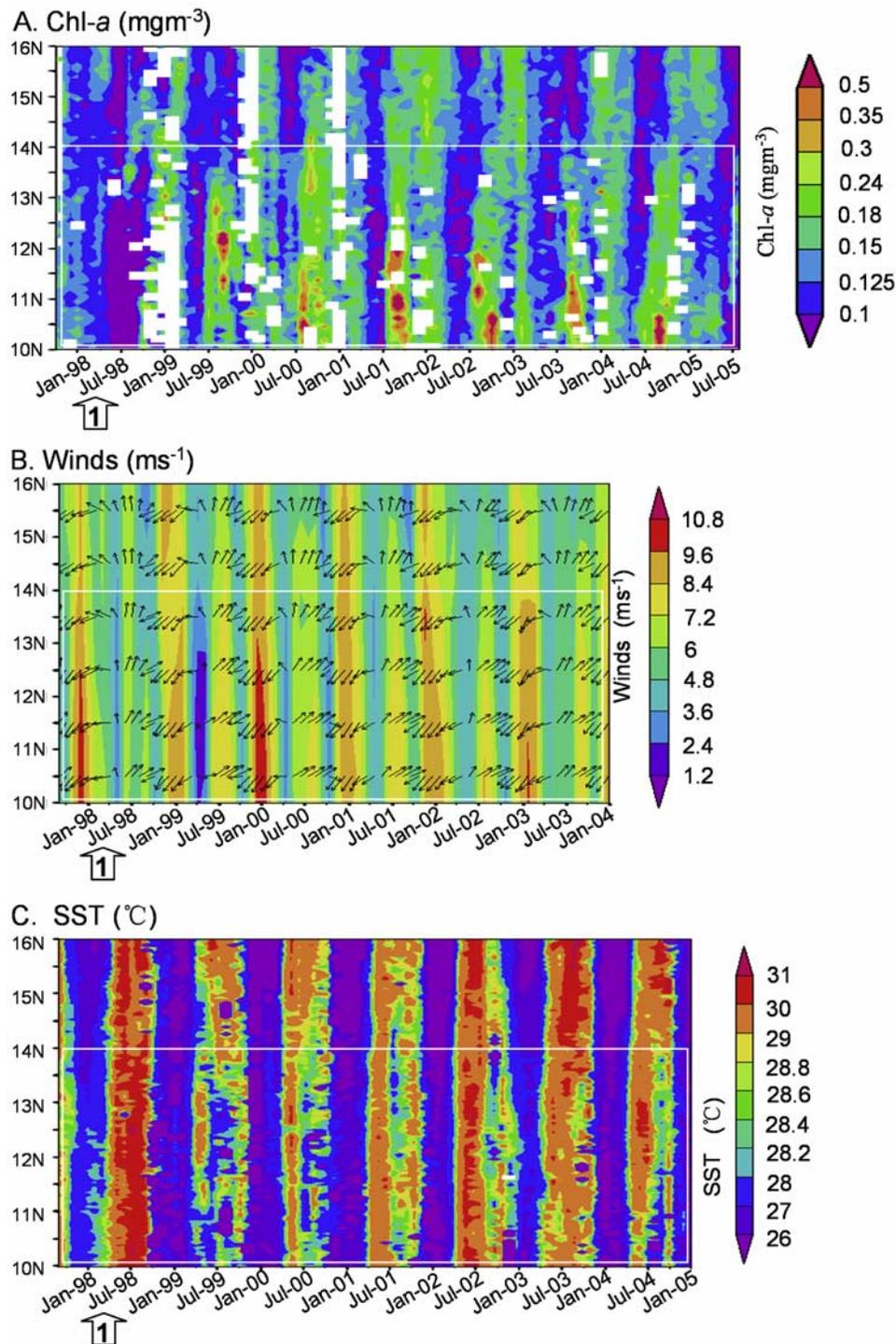
Figure 5. Latitude-time sections data along section T (T in Figure 1b): (a) Chl-*a* from September 1997 to July 2005; (b) NCEP wind from September 1997 to December 2003; (c) AVHRR from September 1997 to December 2004. In Figure 5b, arrows represent only the direction of wind vectors. White bold arrows point to July 1998.

mixed layer. This process may bring rich nutrients from under the euphotic layer. In addition, the strong wind region agrees well with the area of low SST (Figure 4). So the SSWS may also contribute to increasing Chl-*a* concentrations.

[30] The mechanisms determining the spatial and temporal variation in Chl-*a*'' can be summarized as below: (1) In the southeast coast of Vietnam, the coastal wind-derived upwelling and Ekman upwelling, together with an offshore current, may lead to the coastal high Chl-*a* band and offshore jet-shape of high Chl-*a*; (2) In the offshore southeastern SCS, Ekman upwelling induced by strong wind stress curls may cause high Chl-*a* concentrations; (3) In
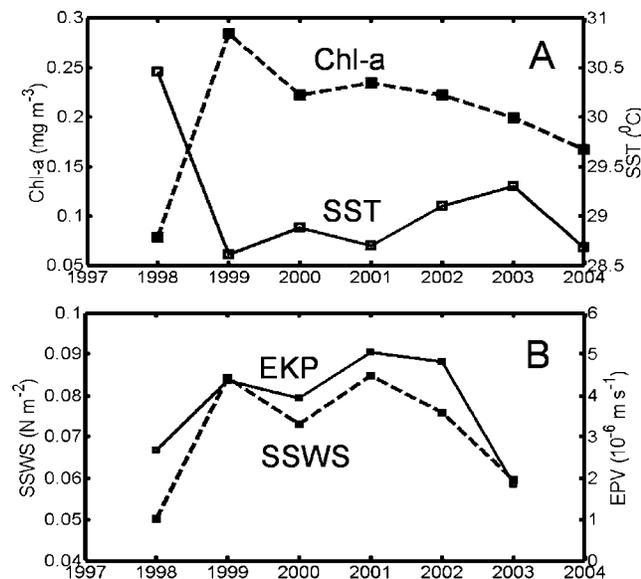
Figure 6. Time series data sampled from box S (Figure 1b) for summer (averaged for 1 June – 31 August) for the period of 1998 to 2004. Chl-*a*; AVHRR SST; NCEP Sea Surface Wind Stress (SSWS); Ekman Pumping Velocity (EPV).

coastal and offshore regions, the direct mixing effect of the strong wind may also enhance the phenomena of high Chl-*a* concentrations.

4.2. Chl-*a* and Oceanic Conditions Along Transect T

[31] Chl-*a* concentrations, wind stress and SST all showed remarkable seasonal and annual cycles in the western SCS (Figures 5a–5c). Chl-*a* concentrations were usually high (≥ 0.12 mg m^{-3}) in summer (June to August) but low (≤ 0.1 mg m^{-3}) in winter or spring. In many tropic marine regions, high Chl-*a* concentrations generally occur in winter and low Chl-*a* concentrations in spring/summer

due to excessively high SST for summer and ample radiation of sunlight for all year [*An and Du*, 2000; *Tang et al.*, 2003; *Zhao et al.*, 2005a]. Compared with nearby areas, relatively lower SST appeared from June to August in this region (a white box between 10–14°N) and indicated the existence of upwelling in the region.

[32] The wind speeds were strong in summer (Figure 5b). Southwest-northeast monsoon winds roughly parallel to the coastline southeast of Vietnam, favorable wind-direction and strong magnitude can lead to coastal upwelling in coastal areas and Ekman upwelling in offshore areas. We found that low Chl-*a* concentrations in summer (Figure 5a) coincided with weak wind and high SST such as in 1998, whereas high Chl-*a* concentrations were associated with strong wind and lower SST such as in 2000. Those observations along transect T again supported the Ekman pumping upwelling hypothesis proposed in section 4.1.

4.3. Low Chl-*a* in 1998 Associated With El Niño

[33] The jet-shape of high Chl-*a* concentrations for summer in the west SCS has been reported in previous studies [*Tang et al.*, 2004a, 2004b]. In the present study we confirmed this jet-shape of high biomass and further observed universally lower Chl-*a* concentrations in 1998 (Figures 2 and 3c). We also reported universally high SST and weak wind speed in 1998 summer (Figures 4 and 6). Figure 6 shows a better relationship among Chl-*a* and SST and other oceanographic data. This relationship indicates that SST may reflect the change in the conditions of nutrients, as a combined effect of SSWS and EKP. The phenomena of the low Chl-*a* concentration, high SST and weak SSWS and EKP are extremely predominant in 1998.

[34] 1997/1998 was the most intense El Niño year in the 20th century. Big differences in ocean circulations were also reported in this year [*Wang et al.*, 2003; *Kuo et al.*, 2004]. The seasonal evolution of ocean surface conditions in the SCS was strongly modulated by the 1997/98 El Niño [*Xie et al.*, 2003; *Liu et al.*, 2004]. The northeast (winter) and southwest (summer) monsoons were weakened due to the
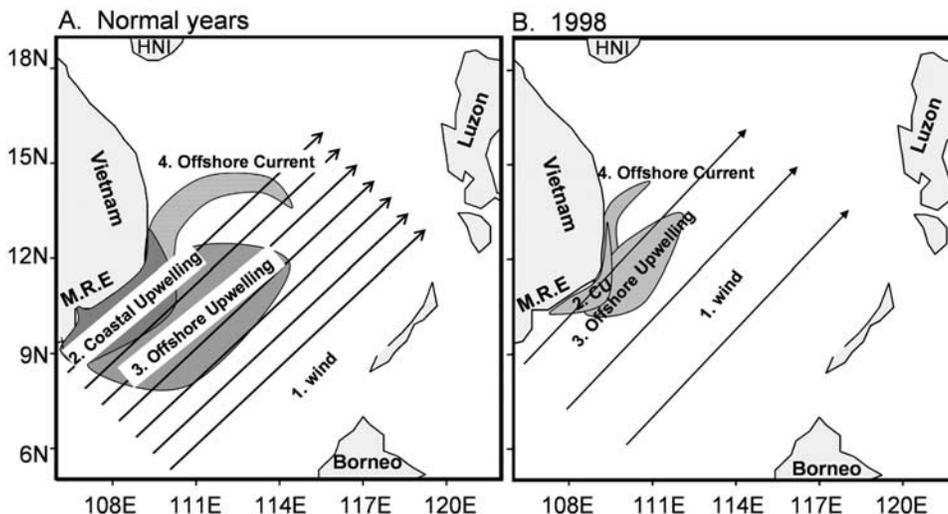
Figure 7. Schematic diagram displaying the mechanism of spatial distribution of Chl-*a* concentration. (1) Strong southwesterly winds; (2) strong coastal upwelling; (3) strong offshore upwelling (Ekman upwelling); (4) large offshore current to the SCS.

El Niño−related shift in atmospheric circulation, resulting in changes (weakening) in wind-driven ocean circulations. The decrease in advection and turbulence of heat flux that associated with the weaker wind speed eventually weakened offshore Ekman upwelling and coastal upwelling.

[35] As we discussed in sections 4.1 and 4.2, Chl-*a* distributions were controlled by wind velocity to a great extent in the western SCS. In 1998, under the influence of El Niño, the weakened coastal wind and the low wind speed in the west of the SCS caused, respectively, the decrease of coastal upwelling alongshore and attenuation of mixing/Ekman upwelling offshore, resulting in lower Chl-*a* concentrations in the western SCS. At the same time, the northward shifting of the weakened offshore current may have reduced offshore transporting intensity of coastal nutrient-rich water, resulting in the weakening of the Chl-*a* jet.

5. Conclusions

[36] The present study revealed a spatial variation of Chl-*a* in the SCS that is reasonably related to oceanic environment and El Niño. High Chl-*a* concentrations in the western SCS were correlated with oceanic conditions, especially the wind stress. The coastal band of high Chl-*a* concentrations and the jet-shape of high Chl-*a* in the western SCS were associated with offshore anticyclonic current and coastal upwelling induced by southwesterly winds. Moreover, the offshore high Chl-*a* concentrations in the western SCS basin were associated with Ekman upwelling induced by eddies of wind stress.

[37] The present study also revealed an annual variation of Chl-*a* in the SCS. In 1998, the El Niño year, unusually high SST, weak wind stress and weak Ekman pumping lead to the decrease of nutrients supporting, resulting in low Chl-*a* concentrations in the summer. We use a conceptual model (Figure 7) to represent summer Chl-*a* distribution in the western SCS for general years (Figure 7a) and 1998 (Figure 7b).

References

Agawin, N. S. R., C. M. Duarte, S. Agusti, and L. McManus (2003), Abundance, biomass and growth rates of *Synechococcus* sp. in a tropical coastal ecosystem (Philippines, South China Sea), *Estuarine Coastal Shelf Sci.*, *56*, 493−502.

An, N. T., and H. T. Du (2000), Studies on phytoplankton pigments: chlorophyll, total carotenoids and degradation products in Vietnamese waters (the South China Sea, area IV), paper presented at 4th Tech. Seminar on Mar. Fish. Resour. Surv. in the South China Sea Area IV: Vietnamese Waters, Southeast Fish. Dev. Cent., Bangkok, 18−20 Sept.

Chu, P. C., C. Fan, C. J. Lozano, and J. L. Kerling (1998), An airborne expendable bathythermograph survey of the South China Sea, May 1995, *J. Geophys. Res.*, *103*, 21,637−21,652.

Hung, T.-C., and C.-H. Tsai (1984), Study on biomass and primary productivity along the southwestern coast of Taiwan, *Acta Oceanogr. Taiwan*, *16*, 8−26.

Kuo, N.-J., Q.-A. Zheng, and C.-R. Ho (2004), Response of Vietnam coastal upwelling to the 1997−1998 ENSO event observed by multi-sensor data, *Remote Sens. Environ.*, *89*, 106−115.

Lau, K.-M., H.-T. Wu, and S. Yang (1998), Hydrologic processes associated with the first transition of the Asian Summer Monsoon: A pilot satellite study, *Bull. Am. Meteorol. Soc.*, *79*, 871−882.

Lee Chen, Y. L., H.-Y. Chen, D. M. Karl, and M. Takahashi (2004), Nitrogen modulates phytoplankton growth in spring in the South China Sea, *Cont. Shelf Res.*, *24*, 527−541.

Lin, I., W. T. Liu, C. Wu, G. T. F. Wong, C. Hu, Z. Chen, W. Liang, Y. Yang, and K. Liu (2003), New evidence for enhanced ocean primary production triggered by tropical cyclone, *Geophys. Res. Lett.*, *30*(13), 1718, doi:10.1029/2003GL017141.

Liu, K.-K., S.-Y. Chao, P.-T. Shaw, G.-C. Gong, C.-C. Chen, and T. Y. Tang (2002), Monsoon-forced chlorophyll distribution and primary production in the South China Sea: observations and a numerical study, *Deep Sea Res., Part I*, *49*, 1387−1412.

Liu, Q., X. Qiang, S. P. Xie, and W. T. Liu (2004), A gap in the Indo-Pacific warm pool over the South China Sea in boreal winter: Seasonal development and interannual variability, *J. Geophys. Res.*, *109*, C07012, doi:10.1029/2003JC002179.

Liu, W.-T., and X. Xie (1999), Space-based observations of the seasonal changes of South Asian monsoons and oceanic response, *Geophys. Res. Lett.*, *26*, 1473−1476.

Shaw, P.-T., and S.-Y. Chao (1994), Surface circulation in the South China Sea, *Deep Sea Res.*, *41*, 1663−1683.

Stewart, R. H. (2002), Response of the upper ocean to winds, in *Introduction to Physical Oceanography*, edited by R. H. Stewart, 152 pp., Dep. of Oceanogr., Tex. A&M Univ., College Station. (Available at http://oceanworld.tamu.edu/resources/ocng_textbook/contents.html)

Tang, D. L., I.-H. Ni, F. E. Müller-Karger, and Z. J. Liu (1998), Analysis of annual and spatial patterns of CZCS-Derived pigment concentrations on the continental shelf of China, *Cont. Shelf Res.*, *18*, 1493−1515.

Tang, D. L., I.-H. Ni, D. R. Kester, and F. E. Müller-Karger (1999), Remote sensing observations of winter phytoplankton blooms southwest of the Luzon Strait in the South China Sea, *Mar. Ecol. Prog. Ser.*, *191*, 43−51.

Tang, D. L., H. Kawamura, M. A. Lee, and T. V. Dien (2003), Seasonal and spatial distribution of Chlorophyll a and water conditions in the Gulf of Tonkin, South China Sea, *Remote Sens. Environ.*, *85*, 475−483.

Tang, D. L., H. Kawamura, T. V. Dien, and M. A. Lee (2004a), Offshore phytoplankton biomass increase and its oceanographic causes in the South China Sea, *Mar. Ecol. Prog. Ser.*, *268*, 31−41.

Tang, D. L., H. Kawamura, H. Doan-Nhu, and W. Takahashi (2004b), Remote sensing oceanography of a harmful algal bloom off the coast of southeastern Vietnam, *J. Geophys. Res.*, *109*, C03014, doi:10.1029/2003JC002045.

Vo, S. T. (1998), The hermatypic Scleractinia of South Vietnam, in *The Marine Biology of the South China Sea*, vol. 3, *Proceedings of the Third International Conference on the Marine Biology of the South China Sea, Hong Kong, 1996*, edited by B. Morton, pp. 11−21, Hong Kong Univ. Press, Hong Kong.

Vo, S. T., and G. Hodgson (1996), Coral reefs of Vietnam: recruitment limitation and physical forcing, paper presented at 8th Int. Coral Reef Symp., Panama City, 24−29 June.

Wang, D. X., Y. Liu, Q. Y. Liu, and P. Shi (2003), Relationships in the upper layer between the Western Pacific Ocean and Indian Ocean during 1997 ∼ 1998 El Niño event (in Chinese), *Prog. Nat. Sci.*, *13*, 957−963.

Wyrtki, K. (1961), Physical oceanography of the south-east Asian waters, in *Scientific Results of Marine Investigations of the South China Sea and the Gulf of Thailand*, pp. 1−195, Scripps Inst. of Oceanogr., La Jolla, Calif.

Xie, S. P., Q. Xie, D. X. Wang, and W. T. Liu (2003), Summer upwelling in the South China Sea and its role in regional climate variations, *J. Geophys. Res.*, *108*(C8), 3261, doi:10.1029/2003JC001867.

Yang, H.-J., and Q. Y. Liu (1998), A summary on ocean circulation study of the South China Sea (in Chinese), *Adv. Earth Sci.*, *13*, 364−368.

Zhao, H., Y. Q. Qi, D. X. Wang, and W. Z. Wang (2005a), Study on the features of chlorophyll-a derived from SeaWiFS in the South China Sea, *Acta Oceanol. Sin.*, *27*, 45−52.

Zhao, H., D. L. Tang, and S. F. Wang (2005b), Spatial distribution of chlorophyll a concentration in summer in western South China Sea and its response to oceanographic environmental factors (in Chinese), *J. Trop. Oceanogr.*, *24*(6), 31−37.

────────────────

D. L. Tang and H. Zhao, Remote Sensing of Marine Ecology and Environment Group (RSMEE), Laboratory for Tropical Marine Environmental Dynamics, South China Sea Institute of Oceanology, and Graduate School of Chinese Academy of Sciences, Chinese Academy of Sciences, 164 West Xingang Road, Guangzhou 510301, China. (lingzistdl@126.com; lingzis@scsio.ac.cn; chaohui@scsio.ac.cn; huizhao1978@163.com)